

Platinum Complexes

Tuning the Aggregation of N^NC Pt(II) Complexes by Varying the Aliphatic Side Chain and Auxiliary Halide Ligand: ¹H and ¹⁹⁵Pt NMR InvestigationMaxim P. Evstigneev,^{*[a,b]} Anastasiya O. Lantushenko,^[a] Yulia A. Yakovleva,^[c] Alfiya F. Suleymanova,^[c] Oleg S. Eltsov,^{*[c]} and Valery N. Kozhevnikov^{*[d]}

Abstract: A series of six tridentate cyclometallated N^NC Pt(II) complexes with different halide auxiliary ligands and different aliphatic side chains have been prepared. All complexes show concentration-dependent NMR spectra. Their self-association was studied by a dilution method monitoring both the ¹H as well as ¹⁹⁵Pt nuclei. Both techniques show similar results validating that ¹⁹⁵Pt NMR is an important methodology to study self-association of potentially any Pt complex regardless of the

nature of the ligands. Experimental data allowed to predict the most probable geometry of the dimers and to get insight into the structural and thermodynamic specificity of the aggregation. The in-depth analysis of the data suggests that the halide auxiliary ligand has no significant influence on self-association while the effect of the aliphatic side chain depends on the length and the structure of the chain.

Introduction

Aggregation and *self*-organisation of square planar Pt(II) complexes is a widely used tool in supramolecular chemistry.^[1] Driven by a variety of intermolecular forces, including metallophilic Pt–Pt interactions, many supramolecular architectures such as gels,^[2,3] liquid crystals^[4–8] and polymers^[9] have been prepared. To study self-aggregation is an important task because the properties of the aggregates are often very different to the ones of individual molecules. For example, photophysical properties are significantly affected by aggregation giving rise to efficient luminescence from aggregated species that is significantly red-shifted in comparison to emission from isolated molecules.^[10] In some cases, non-luminescent Pt complexes produce highly luminescent aggregates in aggregation-induced emission process.^[11–13] The introduction of aliphatic chains is one of the most common tools in the design of liquid crystals

and other soft materials. Usually the tuning of self-organisation is accomplished experimentally by preparing a large series of homologue molecules varying the length of the chains. By studying intermolecular interactions in solution and solid state one can provide more in-depth theoretical understanding of the physical processes involved in self-organisation can be provided and thus inform the design of the materials. In order to build structure-aggregation relationships of Pt(II) complexes it is important to be able to quantify intermolecular interactions.^[14–16] NMR dilution is a very useful technique in this regard. The method is simple and involves measurement of samples at variable concentrations monitoring the change in chemical shifts of protons of the ligands. More recently, ¹⁹⁵Pt NMR has also successfully been used in dilution experiments,^[17] which is an important milestone because ¹⁹⁵Pt NMR methodology can potentially be applied to any Pt complex regardless of the presence or absence of other NMR active nuclei. Indeed, while not every Pt complex contains protons, every Pt complex contains ¹⁹⁵Pt atom. Here we report the ¹H and ¹⁹⁵Pt NMR analysis of self-association of six cyclometallated Pt(II) complexes of NNC type. In particular we evaluated the role of the auxiliary halide ligands and of the aliphatic side chain on *self*-association of these complexes.

Results and Discussions

Structures of the complexes are depicted in Figure 1. The complexes **Pt-Cl**, **Pt-Br** and **Pt-I** have identical tridentate cyclometallating part as well as identical 2-ethylhexyl aliphatic chain but have different halides (Cl, Br, I) as monodentate auxiliary ligands. In this way the role of the auxiliary ligand can be identified. The other three complexes have linear aliphatic chains of

[a] Department of Physics, Sevastopol State University, Sevastopol, 299053, Russian Federation
E-mail: max_evstigneev@mail.ru

<https://sevastopol.su/faces/evstigneev-maksim-pavlovich>

[b] Belgorod State University, 85 Pobedy str., 308015 Belgorod, Russian Federation

[c] Department of Technology for Organic Synthesis, Chemical Technology Institute, Ural Federal University, Yekaterinburg, 620002, Russian Federation
E-mail: o.s.eltsov@urfu.ru
<https://urfu.ru/ru/about/personal-pages/Personal/person/o.s.eltsov/>

[d] Department of Applied Sciences, Northumbria University, Newcastle-Upon-Tyne, NE1 8ST, UK
E-mail: valery.kozhevnikov@northumbria.ac.uk
<https://www.northumbria.ac.uk/about-us/our-staff/k/valery-kozhevnikov/>

Supporting information and ORCID(s) from the author(s) for this article are available on the WWW under <https://doi.org/10.1002/ejic.201900821>.

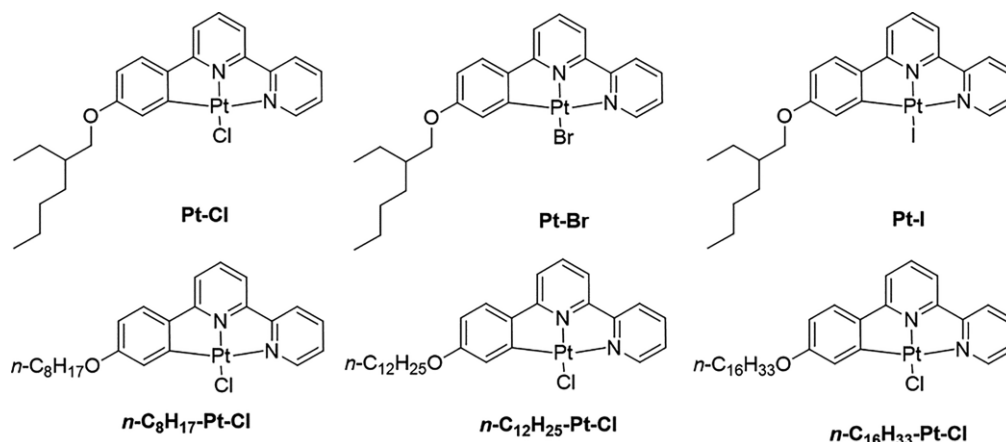


Figure 1. Structures of studied cyclometallated Pt(II) complexes.

different lengths starting from *n*-octyl chain, that is isomeric to branched chain in **Pt-Cl** complex, going further to *n*-docetyl and *n*-hexadecyl chains.

The synthesis of **Pt-Cl** was described previously^[17] and involved the reaction of a corresponding proligand with potassium tetrachloroplatinate in boiling acetic acid. Complexes ***n*-C₈H₁₇-Pt-Cl**, ***n*-C₁₂H₂₅-Pt-Cl** and ***n*-C₁₆H₃₃-Pt-Cl** were synthesized according to the same procedure using corresponding linear alkoxy proligands. The bromocomplex **Pt-Br** and the iodocomplex **Pt-I** were prepared by treating **Pt-Cl** with 10-fold excess of sodium bromide or sodium iodide respectfully. All complexes were characterised by ¹H, ¹³C, ¹⁹⁵Pt NMR and elemental analysis.

In order to carry out NMR dilution studies, solutions of complexes in CDCl₃ were prepared in a range of concentrations from 0.1 mM to 34 mM. Upon decrease of concentration, down-field shift in ¹H NMR spectra was observed in all compounds. This effect was especially strongly manifested for aromatic protons (Figure 2). Interestingly, the opposite effect was observed in ¹⁹⁵Pt NMR and up-field shift of signals for Pt(II) nuclei took place (Figure 3). The set of experimental titration curves and 1D spectra measured for cyclometallated Pt(II) complexes in CDCl₃ using ¹H and ¹⁹⁵Pt NMR nuclei are presented in supplementary information (Figures S1–S9).

Inspection of the $\Delta\delta$ values for each proton in Table 1 suggests that the “a”, “b”, “c”, “d” protons of the pyridine ring appear to be more shielded on average than the “i”, “j”, “h” protons of the benzene ring (see Figure 2). This observation can be explained by the antiparallel structure of the dimer in which the electron-deficient pyridine ring stacks over the electron-rich benzene ring, and the platinum-chloro bonds of the partner molecules in dimer are also antiparallel to each other. Such structure rules out the steric hindrance of the aliphatic side chains in dimer which is crucial for aggregate stability. Interestingly while protons experience shielding upon increase in concentration, platinum nucleus experience small deshielding. The deshielding may be a consequence of a small charge delocalization from the Pt atom due to the action of the above-located large dipole of the Pt-halogen moiety of the partner molecule. Similar deshielding of ¹⁹⁵Pt nucleus was also reported before

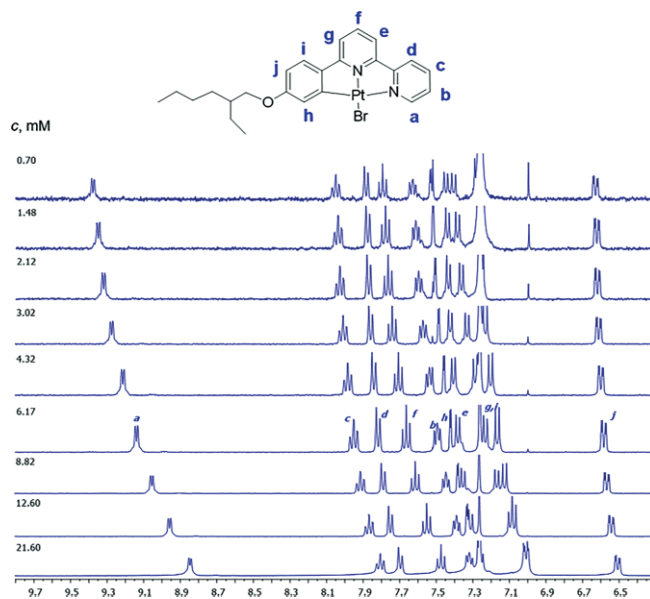


Figure 2. Representative example of NMR dilution experiment. ¹H NMR spectra of **Pt-Br** at different concentrations in CDCl₃ at 298 K.

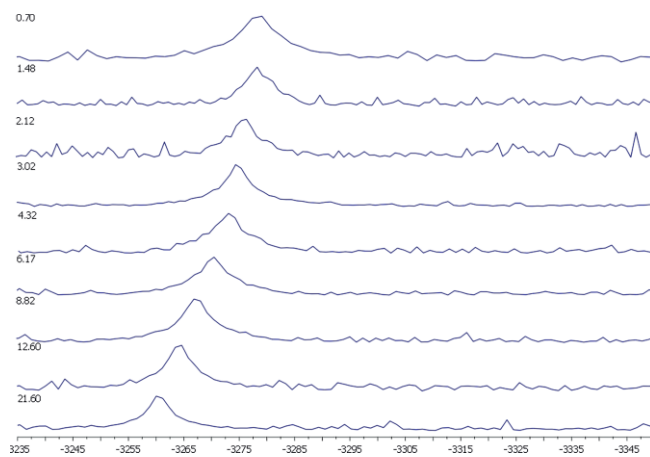


Figure 3. Representative example of NMR dilution experiment. ¹⁹⁵Pt NMR spectra (extracted from 2D ¹H-¹⁹⁵Pt HMBC experiments) of **Pt-Br** at different concentrations in CDCl₃ at 298 K.

Table 1. Calculated aggregation parameters.

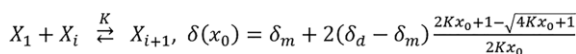
Complex	Nucleus	EK-model		Nucleation model			AK-model	
		<i>K</i> , M ⁻¹	Δ ²	<i>K</i> , M ⁻¹	Δ ²	σ	<i>K</i> , M ⁻¹	Δ ²
Pt-Cl ^[17]	¹ H	44 ± 11	9.5E-05	19 ± 5	7.5E-05	1.8 ± 0.3	30 ± 8	8.1E-05
	¹⁹⁵ Pt	39	0.2	17	0.1	1.6	26	0.2
Pt-Br	¹ H	35 ± 9	5.4E-04	17 ± 3	5.1E-04	1.7 ± 0.3	23 ± 7	5.1E-04
	¹⁹⁵ Pt	45	1.3	19	1.7	1.7	26	1.7
Pt-I	¹ H	25 ± 9	7.3E-04	14 ± 5	6.2E-04	1.4 ± 0.4	16 ± 6	7.6E-04
	¹⁹⁵ Pt	28	0.6	13	0.7	1.8	19	0.7
nC₈H₁₇-Pt-Cl	¹ H	19 ± 5	4.9E-04	11 ± 3	4.9E-04	1.5 ± 0.3	13 ± 6	4.3E-04
	¹⁹⁵ Pt	23	1.7	7	1.8	2.3	11	1.4
nC₁₂H₂₅-Pt-Cl	¹ H	20 ± 6	3.1E-04	10 ± 2	2.8E-04	1.6 ± 0.2	14 ± 6	2.9E-04
	¹⁹⁵ Pt	37	1.0	16	0.9	1.8	22	1.0
nC₁₆H₃₃-Pt-Cl	¹ H	36 ± 8	1.6E-04	20 ± 8	1.4E-04	1.7 ± 0.3	28 ± 7	1.6E-04
	¹⁹⁵ Pt	50	1.5	19	1.3	2.2	35	1.5

for stacking of Pt-containing heterocyclic compounds with nucleotides and also explained by charge delocalization in Pt atom.^[18,19] Noteworthy, the solution study of the self-association of related Pt complex of phenanthroline^[18] also resulted in antiparallel structure, qualitatively similar to that obtained in the present work.

Calculation of the aggregation parameters was accomplished by means of a standard procedure which minimizes the sum of square deviations (Δ² or the discrepancy) of the theoretically calculated chemical shifts from the experimental titration curve, δ(*x*₀), over all concentrations, *x*₀, of the compound *X* measured in experiment for each nucleus studied (Figures S1–S4) (i.e. the data fitting). In order to evaluate the theoretical δ(*x*₀) we used

three different aggregation models reviewed in^[20,21] and accounting for the formation of unrestricted by length aggregates, *X_i*, viz.

(i) indefinite isodesmic model (the EK-model), which assumes that on each aggregation step the equilibrium aggregation constant, *K*, is independent of the number of molecules in aggregate, *i*:



where δ_{*m*} and δ_{*d*} are the chemical shifts of the given nucleus in monomer and dimer, respectively.

Table 2. Calculated proton and ¹⁹⁵Pt chemical shifts.^[a]

nucleus	a	b	c	d	e	f	g	h	i	j	Pt
Pt-Cl											
δ _{<i>m</i>}	9.23	7.67	8.06	7.90	7.45	7.78	7.41	7.34	7.30	6.65	-3467
δ _{<i>d</i>}	8.73	7.37	7.82	7.69	7.18	7.45	7.04	7.08	7.05	6.51	-3450
Δδ	0.50	0.30	0.24	0.21	0.27	0.33	0.37	0.26	0.25	0.14	-17
Pt-Br											
δ _{<i>m</i>}	9.44	7.67	8.07	7.90	7.46	7.83	7.46	7.57	7.32	6.64	-3281
δ _{<i>d</i>}	8.65	7.21	7.67	7.47	6.99	7.28	6.86	7.21	6.90	6.46	-3253
Δδ	0.79	0.46	0.40	0.43	0.47	0.55	0.60	0.36	0.42	0.18	-28
Pt-I											
δ _{<i>m</i>}	9.67	7.58	8.02	7.88	7.46	7.83	7.42	7.89	7.27	6.60	-3499
δ _{<i>d</i>}	9.01	7.17	7.65	7.54	6.99	7.30	6.86	7.50	6.84	6.39	-3475
Δδ	0.66	0.41	0.37	0.34	0.47	0.53	0.56	0.39	0.43	0.21	-24
nC₈H₁₇-Pt-Cl											
δ _{<i>m</i>}	9.22	7.67	8.07	7.89	7.45	7.78	7.41	7.35	7.30	6.65	-3469
δ _{<i>d</i>}	8.51	7.25	7.69	7.50	7.02	7.29	6.83	6.90	6.90	6.43	-3443
Δδ	0.71	0.42	0.38	0.39	0.43	0.49	0.58	0.45	0.40	0.22	-26
nC₁₂H₂₅-Pt-Cl											
δ _{<i>m</i>}	9.21	7.66	8.07	7.89	7.45	7.77	7.40	7.34	7.29	6.64	-3469
δ _{<i>d</i>}	8.56	7.26	7.70	7.52	7.04	7.29	6.87	6.97	6.88	6.42	-3448
Δδ	0.65	0.40	0.37	0.37	0.41	0.48	0.53	0.37	0.41	0.22	-21
nC₁₆H₃₃-Pt-Cl											
δ _{<i>m</i>}	9.21	7.66	8.07	7.89	7.44	7.77	7.40	7.34	7.29	6.64	-3468
δ _{<i>d</i>}	8.74	7.37	7.81	7.65	7.19	7.45	7.02	7.09	7.03	6.51	-3453
Δδ	0.47	0.29	0.26	0.24	0.25	0.32	0.38	0.25	0.26	0.13	-15

[a] The calculated parameters in the table are given for EK-model.

(ii) indefinite nucleation model (or cooperative model) assuming that starting from trimer the K is different from that for dimer by the cooperativity factor, σ , as

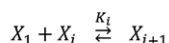
$$K_2 = \sigma K, K_3 = K_4 = \dots = K_i = \dots = K$$

$$x_0 = (1 - \sigma)x_1 + \frac{\sigma x_1}{(1 - Kx_1)^2}, \delta(x_0) = \delta_m + 2(\delta_d - \delta_m) \left[1 - \frac{x_1}{x_0} - \frac{\sigma K x_1^2}{x_0(1 - Kx_1)} \right]$$

where x_1 is the concentration of monomer molecules of X .

Numerical algorithm of the nucleation model solves equation for x_0 with respect to x_1 at each concentration, x_0 , which is further substituted into the equation for $\delta(x_0)$.

(iii) indefinite aggregation model (the AK-model), assuming the intrinsic attenuation of K on aggregate growth due to loss of degrees of freedom



$$x_0 = \sum_{i=1}^{\infty} i x_i, \delta = \delta_m + 2(\delta_d - \delta_m) \left(1 - \frac{x_1}{x_0} - \frac{1}{x_0} \sum_{i=2}^{\infty} x_i \right), K_i = \frac{K_D}{8} \frac{k^3}{(k-1)^3}$$

In this case the numerical algorithm is similar to the nucleation model.

The output of the numerical procedure of data fitting is the set of aggregation parameters, viz. K (or K_D), δ_m , δ_d and σ (only for the nucleation model). The results of computation of the aggregation parameters for the complexes are presented in Table 1 using the three different aggregation models. Table 2 outlines the results of computation of chemical shift values from the EK-model as the most common approach used in literature for comparative analysis of the aggregation parameters.

Comparative Analysis of the ^1H - and ^{195}Pt -Derived Aggregation Parameters

As pointed out earlier, the cyclometallated Pt(II) complexes synthesized in this work provide an opportunity to investigate the application of ^{195}Pt NMR as an alternative or complementary to a widely used ^1H NMR. The obtained values of the mean square deviation (the discrepancy, Δ^2) having the order of 10^{-4} for proton (ca. 0.001 ppm deviation per titration point) and unity for Pt (ca. 0.1 ppm deviation per titration point) evidence good quality of data fitting and reliability of the calculated aggregation parameters. Brief inspection of the calculated values in Table 1 enables to conclude that the parameters derived from ^{195}Pt nucleus are quantitatively similar to that obtained from ^1H derived data for the all three models studied and reveal similar trends. This result is important, suggesting that ^{195}Pt nucleus may be safely used as a probe to quantify the aggregation process of Pt derivatives.

General Characterization of the Aggregation Process

The titration data were acquired in wide concentration range up to 34 mM, which is high enough to expect the formation of aggregates beyond the dimer stage. In such case it was considered reasonable to first apply the isodesmic aggregation model, which takes into account the possibility of formation of formally

indefinite aggregates of the solute molecules with the equilibrium aggregation constant, K , independent of the number i of molecules in each aggregate.^[20,22] The EK-model has so far been acknowledged as the most common approach to investigate the aggregating systems in solution and therefore enables to perform comparative analysis of the K values for different molecules. Another benefit of this model is that, being more general than the alternative dimer aggregation model (which assumes the formation of dimers only and is also often used in the aggregation studies), the EK-model can be simply reduced down to the dimer by dividing the K and multiplying the difference by the factor of two, i.e. $2K_D = K$ and $2(\delta_d - \delta_m) = (\delta_{d(D)} - \delta_{m(D)})$ (see^[23] for review), where “ δ ” stands for the experimental observable chemical shift; “ D ” designates the chemical shift derived from the dimer model; “ d ” and “ m ” stand for the chemical shifts in dimer and monomer, respectively. In more simple words, the aggregation parameters computed using the dimer model can be directly compared with or transformed into the results from the EK-model.^[23,24]

It seen from Table 1 that the equilibrium aggregation constants derived from the EK-model using either the ^1H or ^{195}Pt data can be arranged in the order $K(\text{Pt-Cl}) > K(\text{Pt-I}) > K(\text{Pt-Br})$. The absolute values of K fall in the very narrow range 25–44 M^{-1} suggesting that the aggregation affinity of these complexes in CDCl_3 only weakly depends on the type of halogen atom bound with Pt. It enables to conclude that the specific donor-acceptor intermolecular interactions involving the halogen atom are unlikely to be the main reason for stabilization of the aggregates of the studied molecules in solution. Otherwise the order of K would be correlated with the polarizability of the halogen atom going from **Pt-I** down to **Pt-Cl** as reported previously^[22] or the K dispersion range would be larger due to different strength of Cl/Br/I bonding.^[25] These conclusions are further supported by the calculated values of the induced magnetic shielding of the Pt atom, $\Delta\delta$, outlined in Table 2. The ^{195}Pt chemical shift is known to be very sensitive to ligand attachment spanning in the typical range of dozens ppm when the specific bonds to Pt-halogen framework are being formed.^[26] For our complexes the calculated range of the induced Pt chemical shifts dispersion, $\Delta\delta$, falls within –19 to –28 ppm indicating relatively weak influence of aggregation on electronic environment of ^{195}Pt nucleus.

Next we analysed the influence of the aliphatic side-chain. The data shows that, although the values for $K(\text{nC}_8\text{H}_{17}\text{-Pt-Cl})$ and $K(\text{nC}_{12}\text{H}_{25}\text{-Pt-Cl})$ were approximately the same, there is apparent increase of K for $(\text{nC}_{16}\text{H}_{33}\text{-Pt-Cl})$ as well as for **Pt-Cl**, which is a branched isomer of **nC}_8\text{H}_{17}\text{-Pt-Cl}** (Table 2). Further insight came from the analysis of magnetic shielding, $\Delta\delta$, for either ^1H and ^{195}Pt , which display pronounced changes on going from **nC}_8\text{H}_{17}\text{-Pt-Cl}** to **nC}_{16}\text{H}_{33}\text{-Pt-Cl}** and **Pt-Cl** systematically for all studied nuclei (see Table 2). It follows that the length and the branching of the aliphatic side chain likely affects $\Delta\delta$ through the change in magnetic environment of the studied nuclei, e.g. due to change in ring-current effect (see below). The latter, quite expectedly, will influence the strength of van der Waals dispersive interactions between the molecules in dimers, which, thereby, may explain the above-noted weak depend-

ence of K on the length of aliphatic side chain. The fact that the branched isomer **Pt-Cl** gives the value of K within the same range of magnitudes ($19\text{--}45\text{ M}^{-1}$) as the linear isomer $n\text{C}_8\text{H}_{17}\text{-Pt-Cl}$ may be explained by the contribution from aliphatic chain which hinders the formation of high order aggregates, the effect that was previously reported for variety of aromatic molecules with branched side chains.^[27] To investigate this in more detail, we used nucleation model at which the formation of higher than dimer aggregates occurs with equilibrium constant K differed by the factor of cooperativity of aggregation, σ , from the dimerization constant equal to $\sigma \cdot K$ (see Table 1). It is seen that for either the ^1H or ^{195}Pt -derived results the value of the cooperativity parameter $\sigma > 1$ for all compounds indicating an anticooperative type of the aggregation process. Another contribution to σ may also come from anticooperative factor of the loss of degrees of freedom (intrinsic attenuation of K on aggregate growth) due to aggregate formation.^[21] The aggregation parameters calculated using the AK-model taking into account this factor (see Table 1), display the same or better discrepancy as compared with the EK-model, evidencing that this factor may in principle operate.

The role of side chains and their influence on the character of aggregation may also be viewed by monitoring the concentration dependence of translational diffusion coefficient (D_t , Figure S5) measured for three selected compounds, viz. SAF-08 (branched side chain), SAF-20 (the shortest linear side chain $n\text{C}_8\text{H}_{17}$) and SAF-33 (the longest linear side chain $n\text{C}_{16}\text{H}_{33}$). It is seen that D_t decreases on increasing the concentration evidencing increase of mass of aggregates as a consequence of aggregation. However, the most prominent feature of these data is the asymptotic character of the $D_t(x_0)$ dependences indicating the restriction of the aggregation process beyond the certain aggregate dimensions (if the aggregation would follow the ideal indefinite EK aggregation scheme the D_t should asymptotically approach 0 at infinite concentration). At this stage the estimation of the upper aggregation limit is not possible, however, the obtained results fully support the above-made conclusions regarding the anticooperative influence of aliphatic side chains of Pt(II) complexes regardless their structural specificity (linear or branched).

Structural and Thermodynamic Specificity of the Aggregation Process

Let us refer to Table 2 containing the results of induced proton magnetic shielding, $\Delta\delta$, in dimers using the EK-model. It is seen that independent of the type of halogen atom attached or the length of aliphatic side chain, and the position of the proton in the structure of the molecule, the $\Delta\delta$ values are always positive evidencing the systematic shielding effect of the aggregate formation on the aromatic protons. The obtained average magnitudes of shielding, $\Delta\delta$ ca. $0.3\text{--}0.4$ ppm, are consistent with the ring-current effect originating from diamagnetic shielding induced by delocalized aromatic π -electrons circulating around the aromatic moieties of the molecules, located above each other inside a dimer.^[28] This configuration is possible only for the face-to-face orientation of the molecules in aggregates.^[18,22]

The π -stacked oligomers are known to be stabilized by specific (electrostatic dipolar, donor-acceptor) and non-specific (solvophobic, dispersive van der Waals) interactions.^[22,25,28,29] The analysis of the calculated K and $\Delta\delta$ values performed above, points out that the physical forces driving platinum complexes to each other in aggregates are non-specific, i.e. are manifested on the level of the whole molecule rather than the specific intermolecular atom-atom interactions, and not associated with solvophobic forces. It follows, that dispersive van der Waals interactions are expected to be the leading driving force stabilizing aggregates of the studied Pt(II) complexes. In non-polar solutions such as chloroform the driving force may additionally be modulated by electrostatic dipolar interactions (electrostatic complementarity) of the interacting molecules in aggregates,^[29,30] arranged in a way to minimize the net energy of interaction.

Further insight into the structural and thermodynamic specificity of aggregation of the Pt(II) complexes comes from analysis of calculated magnetic shielding, $\Delta\delta$ (see Table 2). The shielding pattern of the aromatic protons is nearly identical for the studied molecules suggesting that the structures of their aggregates are likely to be similar. If the structures of aggregates are similar, so do the magnitudes of non-specific van der Waals interactions in aggregates (which are dependent on the area of overlap of the molecules in π -stacked complexes^[28]). It explains why the K values are only weakly depended on the type of a halogen or aliphatic chain in the structure. Thus, based on the above-made analysis and following the most recent view on the nature of π -stacking in solutions,^[31] we suggest that van der Waals dispersive interactions between the overlapping aromatic rings in dimers are likely the leading factor stabilizing the aggregates of Pt(II) complexes.

Conclusions

In the present work a series of tridentate $\text{N}^{\wedge}\text{N}^{\wedge}\text{C}$ cyclometalated Pt(II) complexes have been prepared that helped to identify the role auxiliary halide ligands as well as the role of aliphatic side chain play in self-association in solution. Both ^1H and ^{195}Pt NMR show similar results for self-association of $\text{N}^{\wedge}\text{N}^{\wedge}\text{C}$ Pt(II) complexes in CDCl_3 solution, confirming that ^{195}Pt NMR can be successfully used in dilution experiments.

Using the theoretical model treatment of dilution data and the diffusion-ordered NMR spectroscopy data we showed that Pt(II) complexes feature strongly anticooperative character of aggregation originating from the influence of aliphatic side chains which impede the formation of large aggregates. Analysis of the experimental ^1H NMR-titration curves and the calculated aggregation parameters has shown that the complexes are likely to form π -stacked complexes in solution with antiparallel orientation of the partner molecules in dimers, and the nature of the halide auxiliary ligands only weakly influences the aggregation. The attachment of aliphatic chain with different number of carbon atoms results in weak increase in the magnitude of the aggregation constant, either evident for long linear or branched chains. Van der Waals dispersive interactions between the overlapping aromatic rings in dimer are likely to be

the leading factor stabilizing the aggregates while dipolar electrostatic interactions determine the antiparallel structure of the aggregates.

Experimental Section

Materials and Methods.

All solvents and reagents were purchased from Sigma-Aldrich, Acros Organics or Alfa-Aesar and used without further purification unless otherwise specified. NMR spectra were recorded on NMR-Fourier spectrometer "Bruker AVANCE II" (400 MHz for ^1H and 86 MHz for ^{195}Pt) in CDCl_3 . Signal of solvent was used as reference. Ligands were prepared as described previously by alkylation of 2-(pyridin-2-yl)-6-(4-oxyphenyl)pyridine using appropriate bromoalkane.^[17] **Pt-Cl** was synthesized as described previously.^[17]

All DOSY experiments were performed using a double stimulated echo sequence with three spoil gradients with convection compensation (dstegp3s). The diffusion time was $\Delta = 0.05$ s. The delay for gradient recovery was 0.2 ms and the eddy current delay (T_e) was 5 ms. For each DOSY-NMR experiment a series of 11 spectra on 16 K data points were collected. The pulse gradients (g) were incremented from 2 to 95 % of maximum gradient strength in a linear ramp. The temperature was set and controlled at 298 K with an air flow of 535 L h^{-1} in order to avoid any temperature fluctuation due to sample heating during the magnetic field pulse gradients. After Fourier transformation and baseline correction, the diffusion dimension was processed with the Topspin 4.0.5 software. Diffusion coefficients were calculated by Gaussian fits with the T1/T2 software of Topspin.

General procedure for the synthesis of platinum Pt-Cl complexes with n -alkyl chains. The corresponding ligand (0.6 mmol) was dissolved in acetic acid (25 mL). A potassium tetrachloroplatinate (0.6 mmol) was added. The mixture was heated under reflux under argon atmosphere for 18 hours. The mixture was cooled to room temperature and the formed precipitate was filtered off and washed on filter with methanol. The product was then dissolved in DCM and filtered through celite. After evaporation of DCM by rotary evaporation the residue was treated with methanol and the solid product was filtered off.

$n\text{C}_8\text{H}_{17}$ -Pt-Cl Yellow solid. M.p. 185.5–186.5 °C. Yield (135 mg, 47.7 %). ^1H NMR (400 MHz, CDCl_3), (concentration 0.01271 mol/L): $\delta = 8.89$ (1H, d, $J = 5.2$ Hz), 7.94 (1H, td, $J = 7.8, 1.2$ Hz), 7.78 (1H, d, $J = 8.0$ Hz), 7.60 (1H, t, $J = 8.0$ Hz), 7.49 (1H, m), 7.35 (1H, d, $J = 7.6$ Hz), 7.15 (3H, m), 6.58 (1H, dd, $J = 8.4, 2.4$ Hz), 4.06 (2H, t, $J = 6.6$ Hz), 1.78 (2H, m), 1.48 (2H, m), 1.33 (8H, m), 0.90 (3H, t, $J = 6.6$ Hz). ^{13}C NMR (100 MHz, CDCl_3): $\delta = 166.2, 161.1, 157.3, 154.0, 148.7, 145.0, 139.0, 138.4, 138.1, 126.9, 125.9, 122.4, 119.1, 117.7, 116.6, 111.1, 67.9, 31.9, 29.43, 29.38, 29.29, 26.1, 22.7, 14.1$. Elemental analysis calcd. (%) for $\text{C}_{24}\text{H}_{27}\text{N}_2\text{OPtCl}$: C 48.86; H 4.61; N 4.75; found C 48.99; H 4.30; N 4.56.

$n\text{C}_{12}\text{H}_{25}$ -Pt-Cl Yellow solid. M.p. 176–177 °C. Yield (285 mg, 73.6 %). ^1H NMR (400 MHz, CDCl_3), (concentration 0.01935 mol/L): $\delta = 8.81$ (1H, d, $J = 5.2$ Hz), 7.89 (1H, td, $J = 7.8, 1.2$ Hz), 7.75 (1H, d, $J = 8.0$ Hz), 7.56 (1H, t, $J = 8.0$ Hz), 7.44 (1H, m), 7.32 (1H, d, $J = 7.6$ Hz), 7.11 (3H, m), 6.56 (1H, dd, $J = 8.4, 2.4$ Hz), 4.05 (2H, t, $J = 6.6$ Hz), 1.80 (2H, m), 1.48 (2H, m), 1.28 (16H, m), 0.87 (3H, t, $J = 6.6$ Hz). ^{13}C NMR (100 MHz, CDCl_3): $\delta = 166.1, 161.1, 157.3, 153.9, 148.6, 145.1, 138.9, 138.5, 138.1, 126.8, 125.8, 122.5, 119.1, 117.6, 116.7, 111.0, 67.9, 31.9, 29.7, 29.7, 29.7, 29.5, 29.4, 26.4, 26.1, 22.7, 14.1$. Elemental analysis calcd. (%) for $\text{C}_{28}\text{H}_{35}\text{N}_2\text{OPtCl}$: C 52.05; H 5.46; N 4.34; found C 52.25; H 5.33; N 4.14.

$n\text{C}_{16}\text{H}_{33}$ -Pt-Cl Yellow solid. M.p. 179 °C. Yield (145 mg, 48.8 %). ^1H NMR (400 MHz, CDCl_3): $\delta = 8.91$ (1H, d, $J = 5.2$ Hz), 7.95 (1H, td, $J = 7.8, 1.2$ Hz), 7.80 (1H, d, $J = 8.0$ Hz), 7.62 (1H, t, $J = 8.0$ Hz), 7.50 (1H, m), 7.36 (1H, d, $J = 8.0$ Hz), 7.18 (3H, m), 6.58 (1H, dd, $J = 8.4, 2.4$ Hz), 4.06 (2H, t, $J = 6.6$ Hz), 1.80 (2H, m), 1.46 (2H, m), 1.26 (24H, m), 0.88 (3H, t, $J = 6.6$ Hz). ^{13}C NMR (100 MHz, CDCl_3): $\delta = 166.0, 161.1, 157.3, 153.9, 148.5, 145.1, 138.9, 138.5, 138.0, 126.7, 125.8, 122.5, 119.1, 117.6, 116.7, 111.0, 67.9, 31.9, 29.7, 29.7, 29.7, 29.7, 29.7, 29.7, 29.5, 29.4, 29.4, 26.1, 22.7, 14.1$. Elemental analysis calcd. (%) for $\text{C}_{32}\text{H}_{43}\text{N}_2\text{OPtCl}$: C 54.73; H 6.17; N 3.99; found C 54.95; H 6.27; N 3.90.

Pt-Br complex. A mixture of platinum-chlorine complex **Pt-Cl** (100 mg, 0.169 mmol), sodium bromide (174 mg, 1.69 mmol) and 2-ethoxyethanol (10 mL) was heated under reflux under nitrogen atmosphere for 3 hours. The solvent was distilled off under reduced pressure. The residue was purified with a silica gel column chromatography (DCM/MeOH, 50:1) and then recrystallized from MeOH. Yellow solid. M.p. 183 °C. Yield (83 mg, 78 %). ^1H NMR (400 MHz, CDCl_3), (concentration 0.01576 mol/L): $\delta = 8.98$ (1H, dd, $J = 5.2, 0.8$ Hz), 7.88 (1H, td, $J = 7.8, 1.2$ Hz), 7.76 (1H, d, $J = 8.0$ Hz), 7.57 (1H, t, $J = 8.0$ Hz), 7.41 (1H, m), 7.33 (2H, m), 7.11 (1H, d, $J = 8.0$ Hz), 7.08 (1H, d, $J = 7.6$ Hz), 6.55 (1H, dd, $J = 8.4, 2.8$ Hz), 3.93 (2H, dd, $J = 5.6, 2.4$ Hz), 1.74 (1H, m), 1.54–1.35 (8H, m), 0.98–0.91 (6H, m). ^{13}C NMR (100 MHz, CDCl_3): $\delta = 165.8, 161.5, 157.3, 153.7, 149.8, 144.1, 138.8, 138.3, 138.1, 127.0, 125.9, 122.6, 121.4, 117.8, 116.8, 110.7, 70.2, 39.5, 30.6, 29.2, 23.9, 23.1, 14.2, 11.2$. Elemental analysis calcd. (%) for $\text{C}_{24}\text{H}_{27}\text{N}_2\text{OPtBr}$: C 45.43; H 4.29; N 4.42; found C 45.22; H 4.39; N 4.49.

Pt-I complex. A mixture of the chloride complex **Pt-Cl** (100 mg, 0.169 mmol), sodium iodide (253 mg, 1.69 mmol) and 2-ethoxyethanol (10 mL) was heated under reflux under nitrogen atmosphere for 3 hours. The solvent was removed under reduced pressure. The product was purified by silica gel column chromatography (DCM/MeOH, 50:1 as eluent). Yellow solid. M.p. 184 °C. Yield (85 mg, 73.9 %). ^1H NMR (400 MHz, CDCl_3), (concentration 0.01663 mol/L): $\delta = 9.22$ (1H, dd, $J = 5.2, 0.8$ Hz), 7.84 (1H, td, $J = 7.8, 1.2$ Hz), 7.67 (1H, d, $J = 2.4$ Hz), 7.58 (1H, t, $J = 8.0$ Hz), 7.33 (2H, m), 7.09 (1H, d, $J = 8.0$ Hz), 7.06 (1H, d, $J = 8.4$ Hz), 6.51 (1H, dd, $J = 8.4, 2.4$ Hz), 3.914 (2H, dd, $J = 5.6, 2.0$ Hz), 1.75 (1H, m), 1.55–1.35 (8H, m), 0.98–0.92 (6H, m). ^{13}C NMR (100 MHz, CDCl_3): $\delta = 165.0, 161.7, 157.3, 153.4, 152.2, 142.9, 138.5, 138.1, 138.1, 127.2, 126.0, 125.7, 122.9, 118.5, 118.0, 110.5, 70.2, 39.4, 30.6, 29.2, 23.9, 23.1, 14.2, 11.2$. Elemental analysis calcd. (%) for $\text{C}_{24}\text{H}_{27}\text{N}_2\text{OPTI}$: C 42.30; H 3.99; N 4.11; found C 42.51; H 4.10; N 4.31.

Acknowledgments

RFBR is acknowledged for financial support (proj.no.18-03-00232).

Keywords: Pt(II) complexes · Aggregation · Halides · NMR dilution studies · ^{195}Pt NMR

- [1] K. Li, G. S. Ming Tong, Q. Wan, G. Cheng, W.-Y. Tong, W.-H. Ang, W.-L. Kwong, C.-M. Che, *Chem. Sci.* **2016**, *7*, 1653–1673.
- [2] C. A. Strassert, C.-H. Chien, M. D. Galvez Lopez, D. Kourkoulos, D. Hertel, K. Meerholz, L. De Cola, *Angew. Chem. Int. Ed.* **2011**, *50*, 946–950; *Angew. Chem.* **2011**, *123*, 976.
- [3] F. Camerel, R. Ziessel, B. Donnio, C. Bourgoigne, D. Guillon, M. Schmutz, C. Lacovita, J.-P. Bucher, *Angew. Chem. Int. Ed.* **2007**, *46*, 2659–2662; *Angew. Chem.* **2007**, *119*, 2713.

- [4] X. Wu, M. Zhu, D. W. Bruce, W. Zhu, Y. Wang, *J. Mater. Chem. C* **2018**, *6*, 9848–9860.
- [5] V. N. Kozhevnikov, B. Donnio, B. Heinrich, J. A. G. Williams, D. W. Bruce, *J. Mater. Chem. C* **2015**, *3*, 10177–10187.
- [6] V. N. Kozhevnikov, B. Donnio, B. Heinrich, D. W. Bruce, *Chem. Commun.* **2014**, *50*, 14191–14193.
- [7] V. N. Kozhevnikov, B. Donnio, D. W. Bruce, *Angew. Chem. Int. Ed.* **2008**, *47*, 6382–6385; *Angew. Chem.* **2008**, *120*, 6382.
- [8] C. Cuerva, J. A. Campo, M. Cano, C. Lodeiro, *Chem. Eur. J.* **2016**, *22*, 10168–10178.
- [9] J.-F. Mei, X.-Y. Jia, J.-C. Lai, Y. Sun, C.-H. Li, J.-H. Wu, Y. Cao, X.-Z. You, Z. Bao, *Macromol. Rapid Commun.* **2016**, *37*, 1667–1675.
- [10] C.-J. Lin, Y.-H. Liu, S.-M. Peng, T. Shinmyozu, J.-S. Yang, *Inorg. Chem.* **2017**, *56*, 4978–4989.
- [11] L. Ravotto, P. Ceroni, *Coord. Chem. Rev.* **2017**, *346*, 62–76.
- [12] A. Aliprandi, M. Mauro, L. De Cola, *Nat. Chem.* **2016**, *8*, 10–15.
- [13] D. Septiadi, A. Aliprandi, M. Mauro, L. De Cola, *RSC Adv.* **2014**, *4*, 25709–25718.
- [14] K. R. Koch, C. Sacht, C. Lawrence, *J. Chem. Soc., Dalton Trans.* **1998**, *4*, 689–696.
- [15] I. A. Kotzé, W. J. Gerber, J. M. McKenzie, K. R. Koch, *Eur. J. Inorg. Chem.* **2009**, *2009*, 1626–1633.
- [16] V. V. Sivchik, E. V. Grachova, A. S. Melnikov, S. N. Smirnov, A. Y. Ivanov, P. Hirva, S. P. Tunik, I. O. Koshevoy, *Inorg. Chem.* **2016**, *55*, 3351.
- [17] A. F. Suleymanova, O. S. Eltsov, D. N. Kozhevnikov, A. O. Lantushenko, M. P. Evstigneev, V. N. Kozhevnikov, *ChemistrySelect* **2017**, *2*, 3353–3355.
- [18] A. Odani, T. Sekiguchi, H. Okada, S. I. Ishiguro, O. Yamauchi, *Bull. Chem. Soc. Jpn.* **1995**, *68*, 2093–2102.
- [19] T. Yajima, G. Maccarrone, M. Takani, A. Contino, G. Arena, R. Takamido, M. Hanaki, Y. Funahashi, A. Odani, O. Yamauchi, *Chem. Eur. J.* **2003**, *9*, 3341–3352.
- [20] R. B. Martin, *Chem. Rev.* **1996**, *96*, 3043–3064.
- [21] D. A. Beshnova, A. O. Lantushenko, D. B. Davies, M. P. Evstigneev, *J. Chem. Phys.* **2009**, *130*, 04B625.
- [22] U. Mayerhöffer, F. Würthner, *Angew. Chem. Int. Ed.* **2012**, *51*, 5615–5619; *Angew. Chem.* **2012**, *124*, 5713.
- [23] M. P. Evstigneev, A. S. Buchelnikov, V. V. Kostjukov, I. S. Pashkova, V. P. Evstigneev, *Supramol. Chem.* **2013**, *25*, 199–203.
- [24] P. Thordarson in *Supramolecular Chemistry: From Molecules to Nanomaterials*, **2012**.
- [25] P. Metrangolo, G. Resnati, *Chem. Eur. J.* **2001**, *7*, 2511–2519.
- [26] J. Kramer, K. R. Koch, *Inorg. Chem.* **2007**, *46*, 7466–7476.
- [27] M. P. Evstigneev, D. B. Davies, A. N. Veselkov, *Chem. Phys.* **2006**, *321*, 25–33.
- [28] M. P. Evstigneev, *Int. Rev. Phys. Chem.* **2014**, *33*, 229–273.
- [29] M. S. Cubberley, B. L. Iverson, *J. Am. Chem. Soc.* **2001**, *123*, 7560–7563.
- [30] S. L. Cockcroft, C. A. Hunter, K. R. Lawson, J. Perkins, C. J. Urch, *J. Am. Chem. Soc.* **2005**, *127*, 8594–8595.
- [31] H. J. Schneider, *Acc. Chem. Res.* **2015**, *48*, 1815–1822.

Received: July 28, 2019